

Design of linkage mechanisms of partially rigid frames using limit analysis with quadratic yield functions

Makoto OHSAKI¹, Seita TSUDA² and Yuji MIYAZU³

¹ Department of Architecture and Architectural Engineering, Kyoto University
Kyoto-Daigaku Katsura, Nishikyo, Kyoto 615-8540, Japan,
ohsaki@archi.kyoto-u.ac.jp

² Department of Design and Technology, Okayama Prefectural University,
111 Kuboki, Soja 719-1197, Japan

³ Department of Architecture, Hiroshima University, 1-4-1 Kagamiyama,
Higashi-Hiroshima 739-8527, Japan

Abstract

A method is presented for generating linkage mechanisms consisting of frame members. A quadratic programming problem is solved to obtain an infinitesimal mechanism allowing a hinge rotating about an axis in arbitrarily inclined direction. The problem is equivalent to a plastic limit analysis problem with quadratic yield functions with respect to member-end moments and axial force. The directions of hinges are obtained from the ratios of member-end moments along the local axes. A finite mechanism is generated by carrying out geometrically nonlinear analysis and adding hinges, if necessary. Effectiveness of the proposed method is demonstrated through examples of 3-dimensional mechanisms.

Keywords: linkage mechanism, quadratic programming problem, plastic limit analysis, overconstrained mechanism, optimality conditions.

1. Introduction

The methods of designing link mechanisms or linkage mechanisms are classified into analytical approaches (Artobolevsky, 1977; Freudenstein, 1995; Erdman, 1981; Patel and Ananthasuresh, 2007; Yan et al., 2012) and numerical approaches (Root and Ragsdell,

1976). The process of linkage design consists of type synthesis, number synthesis, and path (dimensional) synthesis. Type synthesis determines the type and connectivity of links, number synthesis determines the numbers of links and joints (hinges) to obtain a mechanism with the desired degree of kinematic indeterminacy, and path synthesis finds the locations of hinges and the shapes of links such that the prescribed path is followed by the mechanism.

The path synthesis can be naturally formulated as a nonlinear programming problem to minimize the distance of path of the output node of linkage from the specified path. By contrast, the type synthesis and number synthesis are intrinsically formulated as combinatorial problems that can be solved using an integer programming approach (Zhang et al., 1984; Krishnamurty and Turcic, 1992) or a graph theoretical enumeration method (Kawamoto et al., 2004).

Early studies of systematic procedures for type synthesis can be found in the surveys by Olson et al. (1985) and Erdman (1995). However, it is difficult to solve a combinatorial problem with many variables. It is also important to avoid solutions with large degrees of kinematic indeterminacy. Kim et al. (2007) incorporated a fictitious load and gave a small upper bound for the strain energy. Stolpe and Kawamoto (2005) found mechanisms with single-degree kinematic indeterminacy using the branch-and-bound method. The authors presented a design method of 3-dimensional mechanisms of partially rigid frame based on plastic limit analysis that is formulated as a linear programming problem (Ohsaki et al., 2014; Tsuda et al., 2013a, 2013b). However, in our previous studies, the hinges are restricted to rotate about specified orthogonal axes of local coordinates. Therefore, many hinges including universal joints are needed to generate the desired deformation.

The linkage mechanisms are closely related to developable or expandable structures in the fields of aerospace engineering and architectural engineering (Luo et al., 2008). Mobility of expandable structures are investigated based on symmetry conditions (Kovács et al., 2004; Schulze et al., 2014; Chen et al., 2005). Although the theorems derived using a group theoretic approach are general, they utilize analytical expressions for investigating the properties of small mechanisms.

The kinematic indeterminacy of linkage is computed using the mobility rule (Guest and Fowler, 2005; Schulze et al., 2014) for body-hinge mechanisms, or using the extended Maxwell's rule (Fowler and Guest, 2000) for frames. However, for precise evaluation of

kinematic indeterminacy, especially for an overconstrained mechanism that has zero or negative kinematic indeterminacy derived from the above rules, the rank of compatibility matrix should be computed (Kangwai and Guest, 1999; Liu et al., 2013).

In this paper, we extend our method based on linear programming problem to allow a hinge rotating about an axis in arbitrarily inclined direction from the local coordinates. A limit analysis problem with quadratic yield functions with respect to member-end moments and axial force are solved to generate a partially rigid frame with revolute joints. The directions of hinges are obtained theoretically from the optimality conditions. If extension exists in a member, the member is removed from the frame. The kinematic indeterminacy is defined based on the rank deficiency of the matrix defining equilibrium conditions including the hinge directions. It is shown in numerical examples that 3-dimensional finite mechanisms can be found after carrying out large-deformation analysis and adding some torsional hinges, if necessary, to the infinitesimal mechanism obtained by solving the quadratic programming problem.

2. Outline of method and definition of variables

We consider a linkage consisting of frame members. Although our purpose is to present a method for designing linkage mechanisms, the structure is first modeled as a rigidly-jointed frame that can have perfectly elastoplastic hinges at member-ends. A limit analysis problem based on the lower-bound theorem is solved to find the locations and directions of plastic hinges (Shames and Cozzarelli, 1997). The fully-plastic moment should be applied for rotating members around a plastic hinge. However, we simply replace the plastic hinges by revolute joints of a linkage mechanism rotating without external load. If extension exists in a member, the member is removed from the frame. This way, the plastic collapse mechanism obtained by solving the limit analysis problem turns out to be the infinitesimal mechanism of a linkage (Ohsaki et al., 2014). Large-deformation analysis is carried out to add more hinges, if necessary, to obtain a finite mechanism.

The local member coordinates are defined as shown in Fig. 1(a). The two nodes (member-ends) of member k are denoted by a and b . Axis 1 is directed from node a to

node b , and axes 2 and 3 are the principal axes of the cross-section. The global coordinates are denoted by (x, y, z) .

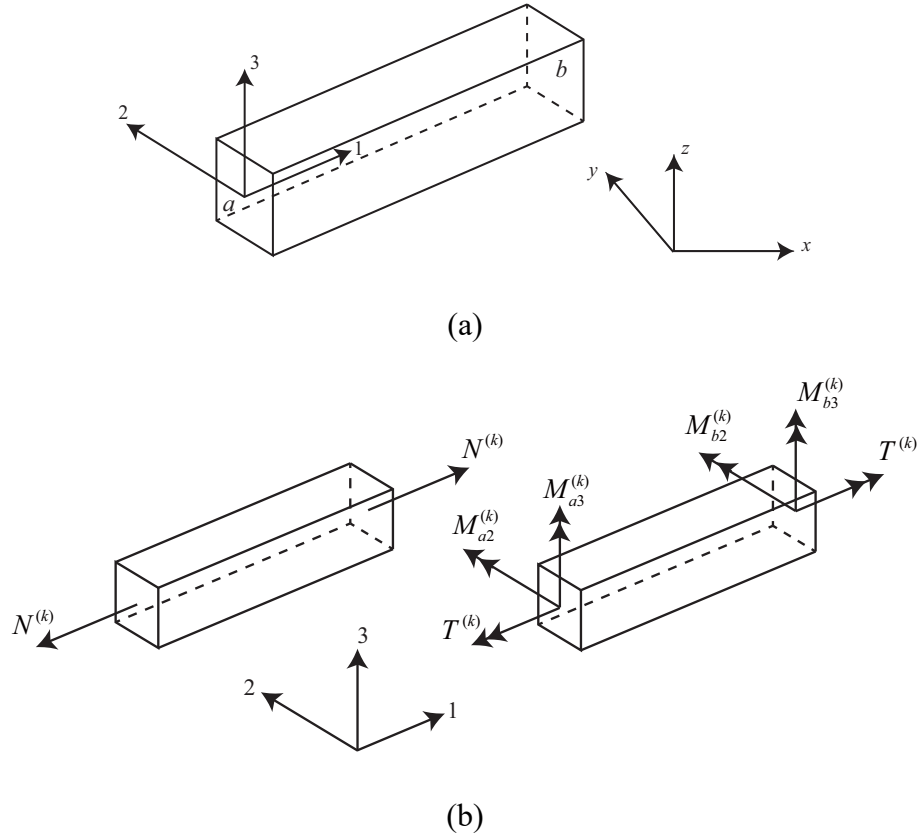


Figure 1: Definition of member coordinates and independent member-end forces; (a) local and global coordinates, (b) six independent member-end forces.

The member-end forces are defined as shown in Fig. 1(b). Let $N^{(k)}$ and $T^{(k)}$ denote the axial force and torsional moment, respectively, of member k . We assume no load is distributed along the member. The axial forces at nodes a and b satisfy the equilibrium condition; therefore, the forces in the direction of axis 1 at nodes a and b have the same magnitude and the opposite directions. Similarly, the torsional moments at nodes a and b have the same magnitude and the opposite directions. The bending moments around axes 2 and 3, respectively, at node $i \in \{a, b\}$ of member k are denoted by $M_{i2}^{(k)}$ and $M_{i3}^{(k)}$. The member-end shear forces in the directions of axes 2 and 3 are eliminated, as functions of bending moments, using the equilibrium equations as described in Appendix

A1. Accordingly, each member has six independent components of member-end forces as shown in Fig. 1(b).

Let $\mathbf{f} = (f_1, \dots, f_{6m})^T$ denote the vector of member-end forces of m members; i.e., each component of \mathbf{f} corresponds to $N^{(k)}$, $M_{a2}^{(k)}$, $M_{a3}^{(k)}$, $M_{b2}^{(k)}$, $M_{b3}^{(k)}$, or $T^{(k)}$ ($k = 1, 2, \dots, m$). The nodal load vector is denoted by $\mathbf{p} = (p_1, \dots, p_n)^T$, where n is the number of degrees of freedom (DOFs) after removing the fixed DOFs. The equilibrium matrix is given as $\mathbf{H} = (\mathbf{h}_1, \dots, \mathbf{h}_{6m})$, where \mathbf{h}_i is defined using the direction cosines of the local axes and member length. \mathbf{H} is obtained by assembling matrices in Eq. (A2) in Appendix of all members, which are transformed to global coordinates. Then the equilibrium equation is written as follows:

$$\mathbf{H}\mathbf{f} = \mathbf{p} \quad (1)$$

The generalized member-end strain vector is denoted by $\mathbf{c} = (c_1, \dots, c_{6m})^T$; i.e., c_i corresponds to member extension and member-end rotations around axes 1, 2, 3, respectively, if f_i is axial force, torsional moment, and bending moments around axes 2 and 3. The vector \mathbf{c} is related to the nodal displacement vector $\mathbf{u} = (u_1, \dots, u_n)^T$ through the compatibility matrix $\mathbf{H}^T = (\mathbf{h}_1, \dots, \mathbf{h}_{6m})^T$ as

$$\mathbf{c} = \mathbf{H}^T \mathbf{u} \quad (2)$$

3. Quadratic programming problem for generating linkage mechanism

Fig. 2 shows an example of planar mechanism, where a filled circle denotes a rotational hinge. By removing two members and adding four hinges, node B moves upward as a result of leftward displacement of node A.

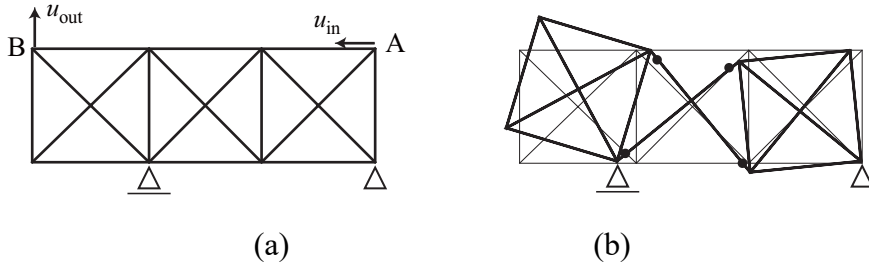


Figure 2: An example of planar mechanism; (a) initial frame, (b) deformation of mechanism.

Since a member-end force is related to one of the components of \mathbf{f} , it is regarded as a function of \mathbf{f} as $N^{(k)}(\mathbf{f})$, $M_{a2}^{(k)}(\mathbf{f})$, $M_{a3}^{(k)}(\mathbf{f})$, $M_{b2}^{(k)}(\mathbf{f})$, $M_{b3}^{(k)}(\mathbf{f})$, or $T^{(k)}(\mathbf{f})$. To generate a mechanism that undergoes a desired deformation by solving a limit analysis problem, input loads are applied at the nodes in the direction of forced deformation, while output loads are applied at the nodes that move in the desired directions. The load vectors that have nonzero values in the components corresponding to the input and output DOFs, respectively, and 0 in other components are denoted by \mathbf{p}_{in} and \mathbf{p}_{out} .

To formulate a plastic limit analysis problem with quadratic yield functions for generating linkage mechanisms, we assign yield functions for member-end moments and axial force, respectively. Upper bounds representing squares of yield axial force and fully plastic moment, respectively, are given for the square of axial force and the sum of squares of three components of moments at each member-end. The optimization problem for maximizing the load coefficient λ_{in} corresponding to the input loads in the presence of output loads is formulated as follows:

$$\begin{aligned}
& \text{maximize } \lambda_{\text{in}} \\
& \text{subject to } \sum_{i=1}^{6m} f_i \mathbf{h}_i = \mathbf{p}_{\text{out}} + \lambda_{\text{in}} \mathbf{p}_{\text{in}} \\
& \quad (T^{(k)}(\mathbf{f}))^2 + (M_{j2}^{(k)}(\mathbf{f}))^2 + (M_{j3}^{(k)}(\mathbf{f}))^2 \leq \alpha w_m, \\
& \quad \quad \quad (k = 1, \dots, m; j \in \{a, b\}) \\
& \quad (N^{(k)}(\mathbf{f}))^2 \leq \alpha w_f, \quad (k = 1, \dots, m)
\end{aligned} \tag{3}$$

where w_m and w_f are the weight coefficients for moment and axial force, respectively, and α is a scaling parameter. Note that our purpose is to generate a mechanism by solving a limit analysis problem. Therefore, the parameters may be artificial, and do not have to represent real properties of the frame. It should also be noted that problem (3) is formulated for the initial undeformed state of the frame; therefore, only infinitesimal mechanism with constant lengths of existing members can be obtained. However, based on our experience, addition of torsional hinges is very effective for converting an infinitesimal mechanism to a finite mechanism.

Let \mathbf{u} , $\gamma_j^{(k)}$ ($j \in \{a, b\}$), and $\gamma_0^{(k)}$ denote the Lagrange multipliers for the first, second, and third constraints, respectively. The Lagrangian Π of problem (3), which is converted to a minimization problem, is formulated as

$$\begin{aligned} \Pi = & -\lambda_{\text{in}} + \left(\mathbf{p}_{\text{out}} + \lambda_{\text{in}} \mathbf{p}_{\text{in}} - \sum_{i=1}^{6m} f_i \mathbf{h}_i \right)^T \mathbf{u} \\ & + \sum_{k=1}^m \sum_{j \in \{a, b\}} \gamma_j^{(k)} \left\{ \left[(T^{(k)}(\mathbf{f}))^2 + (M_{j2}^{(k)}(\mathbf{f}))^2 + (M_{j3}^{(k)}(\mathbf{f}))^2 \right] - \alpha w_m \right\} \\ & + \sum_{k=1}^m \gamma_0^{(k)} \left[(N^{(k)}(\mathbf{f}))^2 - \alpha w_f \right] \end{aligned} \quad (4)$$

The following relations are obtained from the optimality conditions (KKT conditions):

- Normalization of \mathbf{u} :

$$\frac{\partial \Pi}{\partial \lambda_{\text{in}}} = 0 \Rightarrow -1 + \mathbf{p}_{\text{in}}^T \mathbf{u} = 0 \quad (5)$$

- For f_i corresponding to bending moment:

$$\begin{aligned} \frac{\partial \Pi}{\partial M_{jp}^{(k)}} &= 0 \\ \Rightarrow -\mathbf{h}_i^T \mathbf{u} + 2M_{jp}^{(k)}(\mathbf{f}) \gamma_j^{(k)} &= 0, \quad (k = 1, \dots, m; j \in \{a, b\}; p = 2, 3) \end{aligned} \quad (6)$$

- For f_i corresponding to torsional moment:

$$\begin{aligned} \frac{\partial \Pi}{\partial T^{(k)}} &= 0 \\ \Rightarrow -\mathbf{h}_i^T \mathbf{u} + 2T^{(k)}(\mathbf{f})(\gamma_a^{(k)} + \gamma_b^{(k)}) &= 0, \quad (k = 1, \dots, m) \end{aligned} \quad (7)$$

- For f_i corresponding to axial force:

$$\begin{aligned} \frac{\partial \Pi}{\partial N^{(k)}} &= 0 \\ \Rightarrow -\mathbf{h}_i^T \mathbf{u} + 2N^{(k)}(\mathbf{f}) \gamma_0^{(k)} &= 0, \quad (k = 1, \dots, m) \end{aligned} \quad (8)$$

- Complementarity conditions:

$$\begin{aligned} [(T^{(k)}(\mathbf{f}))^2 + (M_{j2}^{(k)}(\mathbf{f}))^2 + (M_{j3}^{(k)}(\mathbf{f}))^2 - \alpha w_m] \gamma_j^{(k)} &= 0, \\ \gamma_j^{(k)} &\geq 0, \quad (k=1, \dots, m; j \in \{a, b\}) \end{aligned} \quad (9)$$

$$[(N^{(k)}(\mathbf{f}))^2 - \alpha w_f] \gamma_0^{(k)} = 0, \quad \gamma_0^{(k)} \geq 0, \quad (k=1, \dots, m) \quad (10)$$

Let $\theta_{jp}^{(k)}$ denote the rotation angle of node j ($\in \{a, b\}$) about the local axis p ($= 1, 2, 3$) of member k , which is a component of the hinge rotation vector. The torsional angle $\theta_1^{(k)}$ around axis 1 is defined as

$$\theta_1^{(k)} = \theta_{b1}^{(k)} - \theta_{a1}^{(k)} \quad (11)$$

From (2), (6), (7), and (11), we have

- Bending:

$$c_i = \mathbf{h}_i^T \mathbf{u} = \theta_{jp}^{(k)} = 2M_{jp}^{(k)} \gamma_j^{(k)}, \quad (k=1, \dots, m; j \in \{a, b\}; p=2, 3) \quad (12)$$

- Torsion:

$$c_i = \mathbf{h}_i^T \mathbf{u} = \theta_1^{(k)} = \theta_{b1}^{(k)} - \theta_{a1}^{(k)} = 2T^{(k)}(\gamma_a^{(k)} + \gamma_b^{(k)}), \quad (k=1, \dots, m) \quad (13)$$

Therefore, the directions of hinges $\mathbf{r}_a^{(k)}$ and $\mathbf{r}_b^{(k)}$ at nodes a and b , respectively, of member k are obtained as follows:

$$\mathbf{r}_a^{(k)} = \begin{pmatrix} \theta_{a1}^{(k)} \\ \theta_{a2}^{(k)} \\ \theta_{a3}^{(k)} \end{pmatrix} = 2\gamma_a^{(k)} \begin{pmatrix} -T^{(k)} \\ M_{a2}^{(k)} \\ M_{a3}^{(k)} \end{pmatrix}, \quad \mathbf{r}_b^{(k)} = \begin{pmatrix} \theta_{b1}^{(k)} \\ \theta_{b2}^{(k)} \\ \theta_{b3}^{(k)} \end{pmatrix} = 2\gamma_b^{(k)} \begin{pmatrix} T^{(k)} \\ M_{b2}^{(k)} \\ M_{b3}^{(k)} \end{pmatrix} \quad (14)$$

i.e., the components of rotation vector at a member-end are proportional to the bending and torsional moments.

Note again that the parameters for limit analysis are artificial, and do not have to represent the real yield force or fully plastic moments. Furthermore, the plastic hinge and member-end moment do not have to be co-axial in the process of plastic limit analysis of a frame. However, it is important to confirm that the direction of the hinge is obtained from Eq. (14) to find the hinge direction of a mechanism.

This way, the direction of a hinge is obtained by solving the quadratic programming problem, and a mechanism with inclined hinges is generated. Note from (9) that $\gamma_j^{(k)}$ vanishes and no hinge is generated, if the yield condition for the moments is not satisfied with equality. A member is to be removed if member extension exists, i.e., $\gamma_0^{(k)} \neq 0$.

The following auxiliary quadratic programming problem is solved to find a lower bound of the parameter α in a similar manner as Ohsaki *et al.* (2014):

$$\begin{aligned}
& \text{maximize } \mu \\
& \text{subject to } \sum_{i=1}^{6m} f_i \mathbf{h}_i = \mu \mathbf{p}_{\text{out}} \\
& (T^{(k)}(\mathbf{f}))^2 + (M_{j_2}^{(k)}(\mathbf{f}))^2 + (M_{j_3}^{(k)}(\mathbf{f}))^2 \leq w_m, \quad (k = 1, \dots, m; j \in \{a, b\}) \\
& (N^{(k)}(\mathbf{f}))^2 \leq w_f, \quad (k = 1, \dots, m)
\end{aligned} \tag{15}$$

Let $\hat{\mu}$ denote the optimal objective value of problem (15). The member-end forces of the optimal solution are also denoted by a hat. Equilibrium equation is written as

$$\frac{1}{\hat{\mu}} \sum_{i=1}^{6m} \hat{f}_i \mathbf{h}_i = \mathbf{p}_{\text{out}} \tag{16}$$

which leads to an obvious relation that the member-end forces for \mathbf{p}_{out} are $1/\hat{\mu}$ of those for $\hat{\mu}\mathbf{p}_{\text{out}}$. Since the left-hand-sides of the inequality constraints of problem (15) are increasing functions of the member-end forces, some of the inequality constraints are satisfied with equality at the optimal solution. Let K_m and K_f denote the sets of such constraints for moments and axial forces, respectively, i.e.,

$$\begin{aligned}
& (\hat{T}^{(k)}(\hat{\mathbf{f}}))^2 + (\hat{M}_{j_2}^{(k)}(\hat{\mathbf{f}}))^2 + (\hat{M}_{j_3}^{(k)}(\hat{\mathbf{f}}))^2 = w_m, \quad (k \in K_m; j \in \{a, b\}) \\
& (\hat{N}^{(k)}(\hat{\mathbf{f}}))^2 = w_f, \quad (k \in K_f)
\end{aligned} \tag{17}$$

We denote the member-end forces for \mathbf{p}_{out} by a tilde, i.e., $\tilde{\mathbf{f}} = (1/\hat{\mu})\hat{\mathbf{f}}$. Then, the following relations hold:

$$\begin{aligned}
(\tilde{T}^{(k)}(\tilde{\mathbf{f}}))^2 + (\tilde{M}_{j_2}^{(k)}(\tilde{\mathbf{f}}))^2 + (\tilde{M}_{j_3}^{(k)}(\tilde{\mathbf{f}}))^2 &= \frac{1}{\hat{\mu}^2} w_m, \quad (k \in K_m; j \in \{a, b\}) \\
(\tilde{N}^{(k)}(\tilde{\mathbf{f}}))^2 &= \frac{1}{\hat{\mu}^2} w_f, \quad (k \in K_f)
\end{aligned} \tag{18}$$

Therefore, if $\alpha = 1/\hat{\mu}^2$ is assigned in problem (3) without input loads, i.e., $\lambda_m = 0$, then the member-end forces $\tilde{\mathbf{f}}$ satisfy the inequality constraints in the sets K_m and K_f of problem (3) with equality. Hence, $\alpha = 1/\hat{\mu}^2$ ensures existence of a feasible solution in problem (3). This way, a conservative lower bound of α is obtained as $\alpha^L = 1/\hat{\mu}^2$, which means that a feasible solution of problem (3) may exist even for α that is less than α^L , if the absolute values of left-hand-sides of all constraints in K_m and K_f decrease as λ_m is increased from 0.

By solving the limit analysis problem (3), a collapse mechanism is obtained; therefore, a linkage mechanism can be obtained by replacing a plastic hinge by a revolute joint. Since the mechanism considered here is a bar-and-joint system, the degree of kinematic indeterminacy is computed using the standard approach for bar-and-joint systems, rather than the mobility rule of linkage.

Let \hat{m} denote the number of members after removing those with nonzero extensional strain in the solution of problem (3). The number of joints including the supports after removing the unnecessary members, the number of constrained DOFs at supports, and the number of released DOFs, which is equal to the number of hinges are denoted by \hat{j} , k , and d , respectively. Then, the degree of kinematic indeterminacy of mechanism, denoted by q , is calculated as

$$q = 6\hat{j} - 6\hat{m} + d - k \tag{19}$$

Alternatively, the degree of kinematic indeterminacy can be computed using the rank of the equilibrium matrix. Suppose \mathbf{H} represents the equilibrium matrix after removing the rows corresponding to the fixed DOFs and the columns corresponding to the member-end forces and moments of non-existing members, which are also removed from the member-end force vector \mathbf{f} . For an inclined hinge in the direction of $\mathbf{r}_a^{(k)}$ at node a of

member k , the condition for the corresponding vector of member-end moments $\mathbf{f}_a^{(k)}$ is written as

$$\mathbf{r}_a^{(k)T} \mathbf{f}_a^{(k)} = 0 \quad (20)$$

A similar relation can be formulated for node b . The conditions (20) for all hinges are assembled as $\mathbf{R}^T \mathbf{f} = \mathbf{0}$, which leads to the equilibrium equations of the structure with hinges as

$$\mathbf{G} \mathbf{f} = \mathbf{0} \quad (21)$$

where

$$\mathbf{G} = \begin{pmatrix} \mathbf{H} \\ \mathbf{R} \end{pmatrix} \quad (22)$$

Let g_r and g_c denote the numbers of rows and columns, respectively, of matrix \mathbf{G} . The rank r of the rectangular matrix \mathbf{G} is computed by carrying out singular value decomposition. The degrees of statical indeterminacy and kinematic indeterminacy are obtained from $g_c - r$ and $g_r - r$, respectively.

4. Numerical examples

Mechanisms with inclined joints are generated to demonstrate the validity of the proposed method. In the following examples, the units of force and length are N and m, respectively, which are not written explicitly, because the size of frame model can be scaled arbitrarily, and no force is needed for deformation of a linkage mechanism. The optimization library SNOPT Ver. 7.2 (Gill et al., 2002) is used for solving the quadratic programming problem. Singular value decomposition of matrix \mathbf{G} is carried out using MATLAB R2013a (MathWorks, 2013)

Since only small deformation is considered in the process of generating a mechanism by solving the optimization problem (3), ABAQUS Ver. 6.13 (Dassault Systèmes, 2014) is used for investigating the properties in large-deformation range. Geometrically nonlinear pseudo-static analysis is carried out by increasing the path parameter t , which represents an input displacement component of each model, from 0 to 1 corresponding to initial and final configurations, respectively. The material is steel with Young's modulus

200 GPa, and each member is divided into two beam elements. The zero-length element called CONN3D2 is used with hinge property representing the revolute joint. The units of force and length are shown in the results of geometrically nonlinear analysis.

Model 1

We first consider a simple four-bar model as shown in Fig. 3(a), where the numbers with and without parentheses are member and node numbers, respectively. Each member has the unit length. All translational and rotational displacement components except z -directional displacement are constrained at node 1, and z -directional displacement is constrained at nodes 2, 3, 4, and 5.

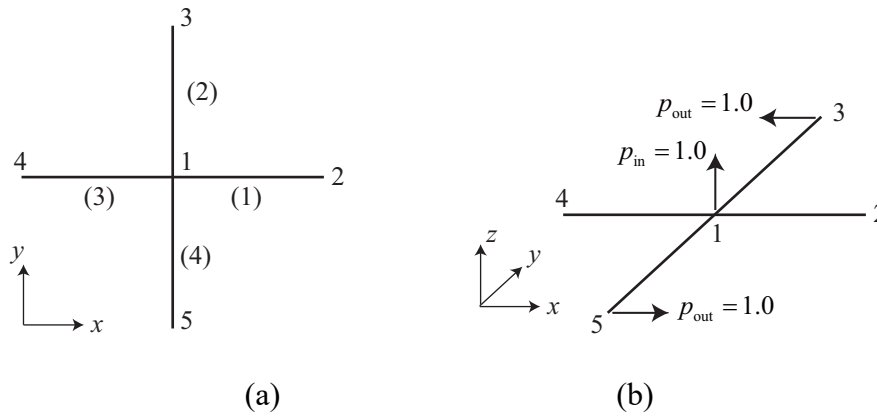


Figure 3: A simple four-bar model (Model 1): (a) plan view and node/member numbers, (b) diagonal view and input/output loads.

A mechanism is obtained so that the output nodes 3 and 5 move to left and right, respectively, as a result of pulling the input node 1 in z -direction. For this purpose, the input load is given at node 1, and the output loads are applied at nodes 3 and 5, as shown in Fig. 3(b). The weight coefficients w_m and w_f are 10.0 and 1000.0, respectively. A large value is given for w_f , because member removal is not necessary for this model. The problem (15) is solved to find the load factor $\hat{\mu} = 3.1622$; i.e., $\alpha^L = 1 / (3.1622)^2 = 0.1000$.

Optimization problem (3) is solved to find the hinge locations as indicated with thick lines in Fig. 4(a). Suppose the local axis 1 is directed from the center node (node 1) for

all members. The hinges of members 2 and 4 at node 1 are inclined as shown in Fig. 4(b) and (c), while those of members 1 and 3 are directed to axis 2 as shown in Fig. 4(c).

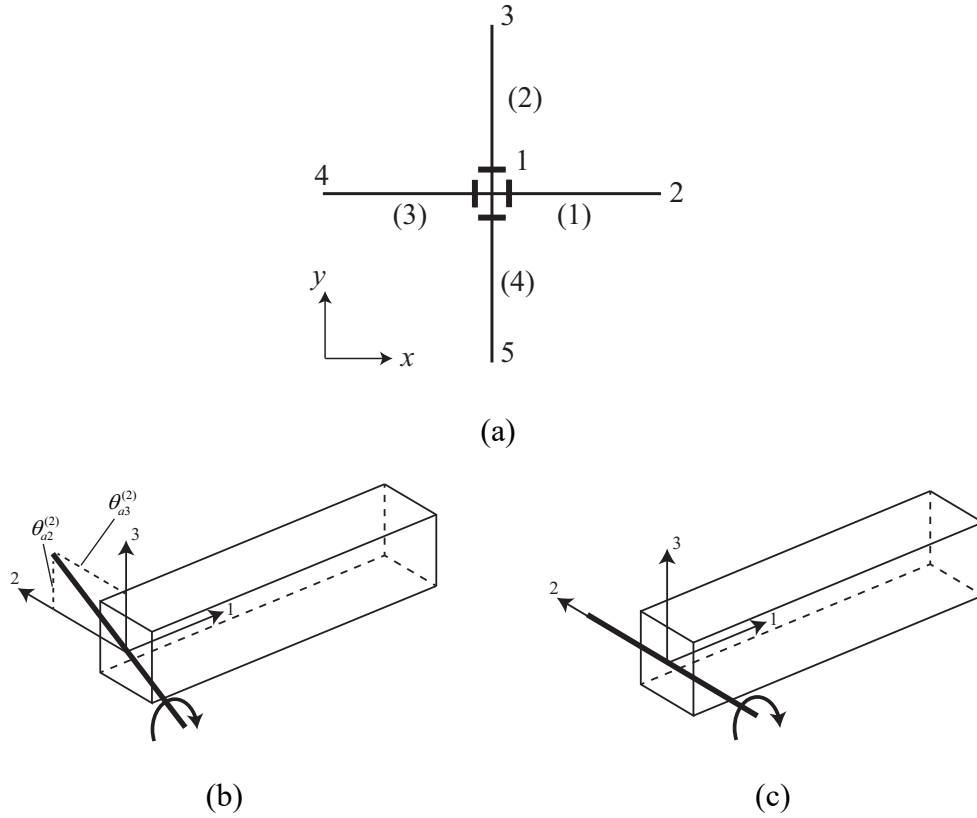


Figure 4: Locations and directions of hinges of Model 1; (a) hinge locations, (b) direction of hinges of members 2 and 4, (c) direction of hinges of members 1 and 3.

The degree of inclination varies with the parameter α . The values of $M_{a_2}^{(2)}$, $M_{a_3}^{(2)}$, $\theta_{a_2}^{(2)}$, and $\theta_{a_3}^{(2)}$ for $\alpha = 0.2, 0.4, \text{ and } 0.6$ are listed in Table 1. The value of $T^{(2)}$ is omitted, because it vanishes for all cases. Note that $M_{a_2}^{(2)}$ and $M_{a_3}^{(2)}$ are obtained directly from the optimal values of variables, and $\theta_{a_2}^{(2)}$ and $\theta_{a_3}^{(2)}$ are computed from the nodal displacements \mathbf{u} , which are obtained as the Lagrange multipliers, and the compatibility equations (2). It is confirmed that $\theta_{a_3}^{(2)} / \theta_{a_2}^{(2)} = M_{a_3}^{(2)} / M_{a_2}^{(2)}$ is satisfied so that the axis of rotation of the hinge coincides with the axis of bending moment of the plastic hinge.

Table 1: Values of $M_{a_2}^{(2)}$, $M_{a_3}^{(2)}$, $\theta_{a_2}^{(2)}$, and $\theta_{a_3}^{(2)}$ for $\alpha = 0.2, 0.4$, and 0.6 of Model 1.

α	$M_{a_2}^{(2)}$	$M_{a_3}^{(2)}$	$\theta_{a_2}^{(2)}$	$\theta_{a_3}^{(2)}$
0.2	-1.00000	-1.00000	-1.00000	-1.00000
0.4	-1.73205	-1.00000	-1.00000	-0.57735
0.6	-2.23607	-1.00000	-1.00000	-0.44721

The values of \hat{m} and \hat{j} are 4 and 5, respectively. One DOF is constrained at each of supports 2–5, and five DOFs are constrained at node 1, i.e., $k = 9$. Four DOFs are released around node 1, i.e., $d = 4$. Therefore, the value of q obtained from Eq. (19) is $6 \times 5 - 6 \times 4 + 4 - 9 = 1$. The values of g_r , g_c , and r are 25, 24, and 24, respectively; i.e., the structure has single-degree kinematic indeterminacy.

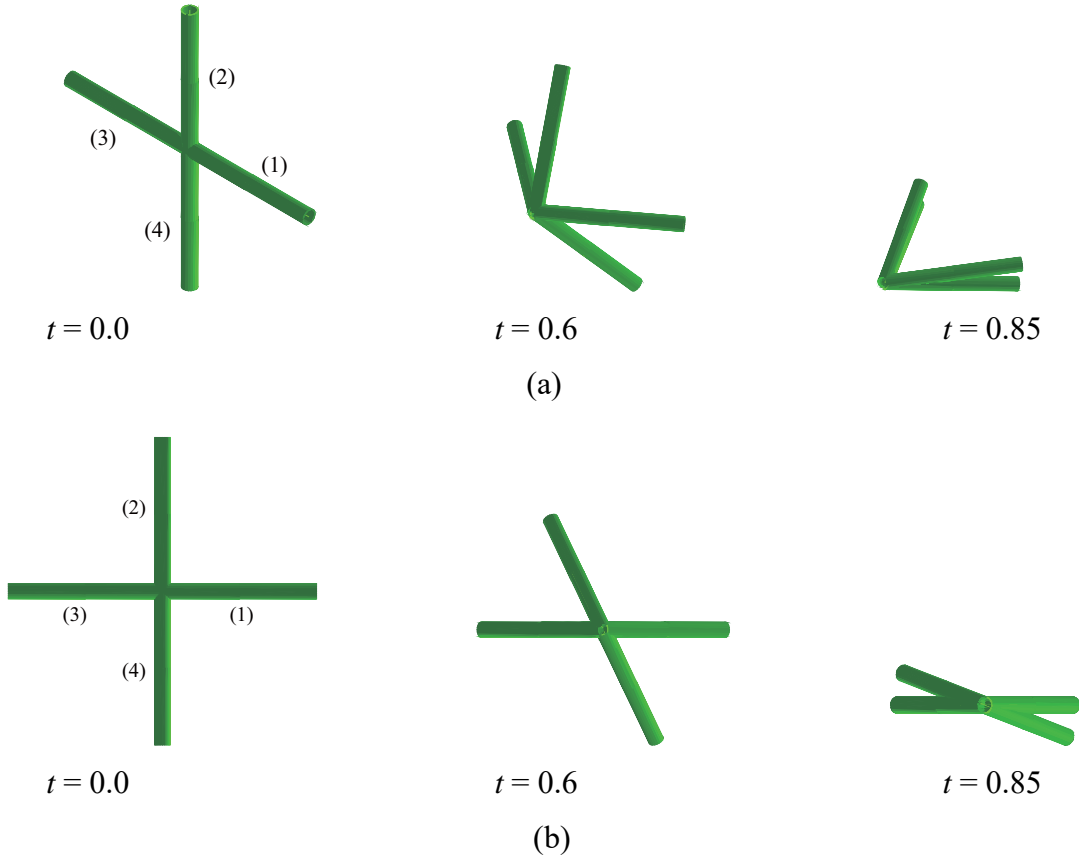


Figure 5: Deformation process of Model 1 ($\alpha = 0.4$); (a) diagonal view, (b) top view.

Large-deformation analysis is carried out using ABAQUS. Each member has pipe cross-section with radius 50 mm and thickness 2 mm. In this example, the value of t corresponds to the z -directional displacement at node 1, which is regarded as the input displacement. The deformation process for $\alpha = 0.4$ is shown in Fig. 5. It is seen from Fig. 5(b) that members 2 and 4 rotate about node 1.

The relation between the input displacement t and the z -directional reaction force at node 1 is plotted in Fig. 6. The solid, dotted, and chained lines correspond to $\alpha = 0.2$, 0.4, and 0.6, respectively. It is seen from the figure that no force is needed until the input displacement t , which is equal to the height of node 1, reaches the values 0.707, 0.866, and 0.913, respectively, for $\alpha = 0.2$, 0.4, and 0.6.

Let ζ denote the angle of the hinge direction vector from the x -axis at node 1 of member 2, e.g., for $\alpha = 0.2$, $\tan \zeta = 1.0/1.0 = 1.0$ leads to $\zeta = \pi/4$. We can see that member 2 exist in xz -plane when $t = \cos \zeta = 0.707$, because the length of member 2 is 1.0. Therefore, node 3 should be released from xy -plane when t is increased further from 0.707. Since we assume elastic material for the members, the reaction force becomes nonzero as t approaches 1 as seen in Fig. 6.

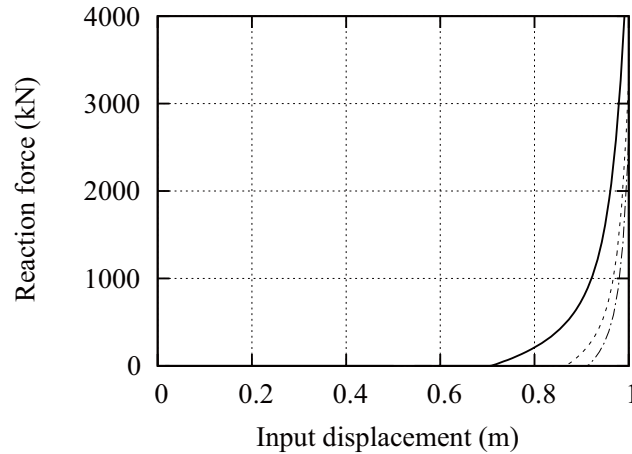


Figure 6: Relation between z -directional input displacement at node 1 and corresponding reaction force of Model 1; solid line: $\alpha = 0.2$, dotted line: $\alpha = 0.4$, chained line: $\alpha = 0.6$.

The relation between t and the x -directional displacement at node 5, which is regarded as the output displacement, is plotted in Fig. 7. The solid, dotted, and chained lines correspond to $\alpha = 0.2, 0.4$, and 0.6 , respectively. It is seen from the figure that the output displacement increases as members 2 and 4 rotate around node 1; however, it decreases as four members become close to the vertical axis. The maximum output displacements are calculated as $\sin \zeta$, which are $0.707, 0.500$, and 0.408 for $\alpha = 0.2, 0.4$, and 0.6 , respectively. The model for $\alpha = 0.2$ has the largest output displacement, because the direction of the hinge axis is closest to z -direction among three cases.

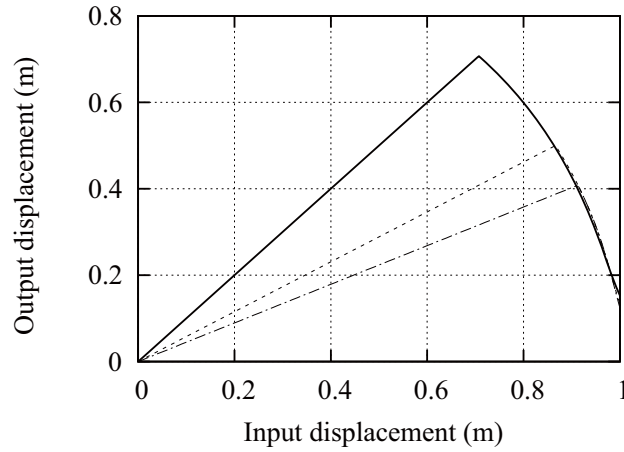


Figure 7: Relation between z -directional input displacement at node 1 and x -directional output displacement at node 5 of Model 1; solid line: $\alpha = 0.2$, dotted line: $\alpha = 0.4$, chained line: $\alpha = 0.6$.

Model 2

We next consider a square grid with unit member length as shown in Fig. 8. Nodes 2 and 4 are supported in y - and z -directions, and nodes 3 and 5 are supported in x - and z -directions. The weight coefficients w_m and w_f are 10.0 and 1000.0 , respectively, also for this model. A mechanism is generated so that the output nodes 6–9 move in z -direction as a result of pulling the input node 1 in negative z -direction. Problem (15) is solved to find the load factor $\hat{\mu} = 8.6395$; therefore, $\alpha^L = 1/(8.6395)^2 = 0.01340$.

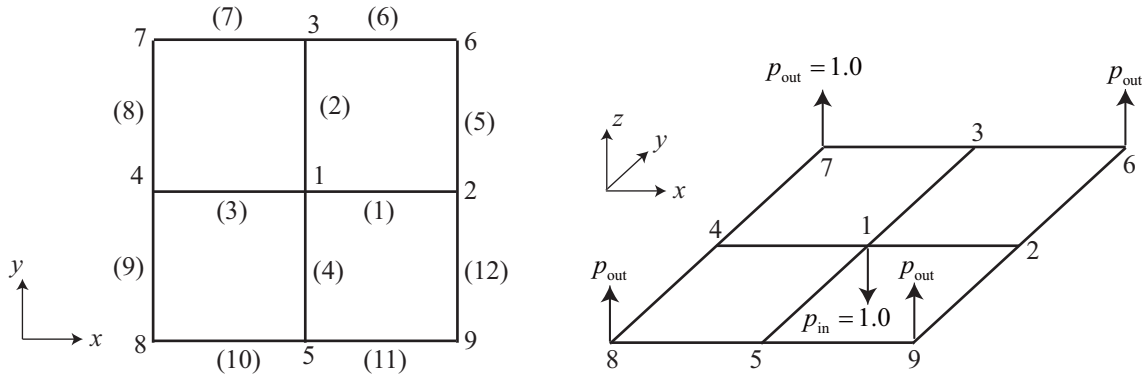


Figure 8: A simple square-grid model (Model 2): (a) plan view and node/member numbers , (b) diagonal view and input/output loads.

The input and output loads are applied at the input and output nodes, respectively, to solve problem (3) for $\alpha = 0.1$. However, we found that the number of hinges is too small, if problem (3) is simply solved. Therefore, the z -coordinate of node 1 is decreased by 0.01 and the z -coordinates of nodes 6–9 are increased by 0.01 to generate the hinges as indicated with thick lines in Fig. 9(a). The directions of hinges in global coordinates at the connections of member 5 to nodes 2 and 6 (nodes a and b of member 5) are listed in Table 2. As seen from the table, various hinge directions are obtained by varying the parameter α .

Table 2: Directions of hinges in global coordinate system at the connection of member 5 to nodes 2 and 6 of Model 2.

α	Node 2 (node a of member 5)			Node 6 (node b of member 5)		
	x	y	Z	x	y	Z
0.1	0.91137	0.41137	0.01336	0.41137	0.41137	-0.81336
0.2	1.20711	0.70711	0.20711	0.70711	0.70711	-1.00000
0.3	1.36603	0.86603	0.61966	0.86603	0.86603	-1.22474

Large-deformation analysis is carried out using ABAQUS. Each member has pipe cross-section with radius 50 mm and thickness 2 mm. Relation between negative z -directional input displacement at node 1 and corresponding reaction force is plotted in Fig. 10, which indicates that this mechanism is not a finite mechanism. Therefore, we

added eight torsional hinges as indicated with \times in Fig. 9(b) to generate a finite mechanism. Note that a torsional hinges can be placed at anywhere along the member with the same effect.

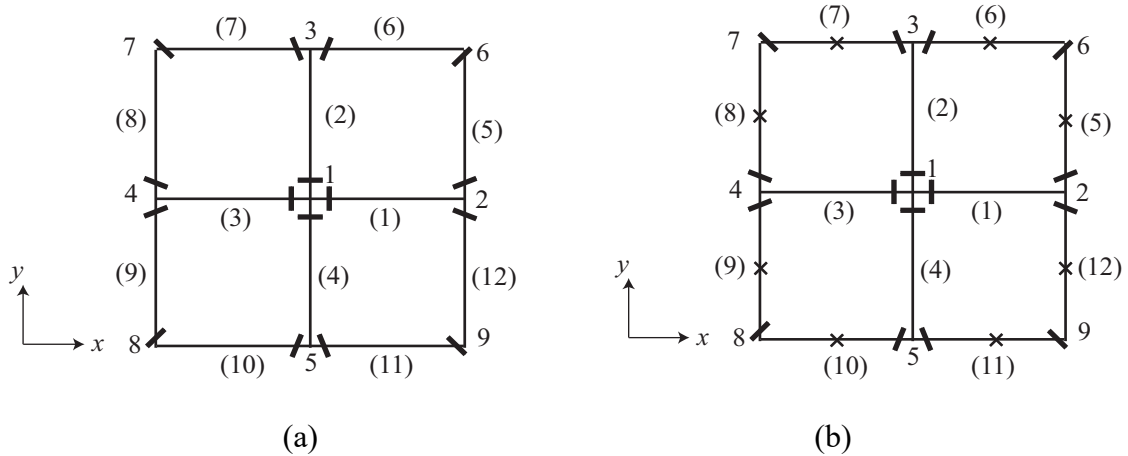


Figure 9: Locations of hinges of Model 2; (a) infinitesimal mechanism obtained by solving problem (3), (b) finite mechanism after adding eight torsional hinges.

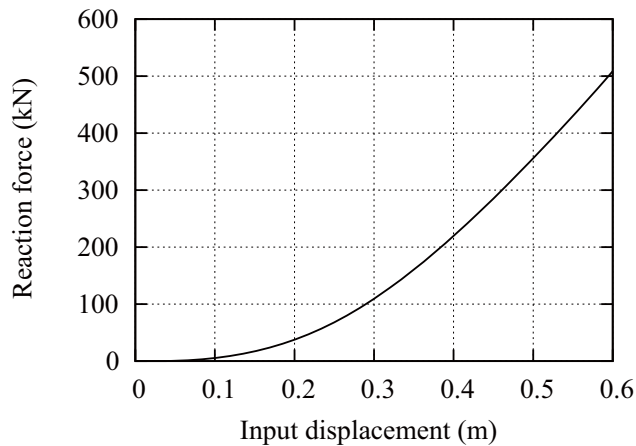


Figure 10: Relation between z -directional input displacement at node 1 and corresponding reaction force of Model 2 ($\alpha = 0.1$) before adding torsional hinges.

The deformation process is shown in Fig. 11 for $\alpha = 0.1$. Nodes 6–9 move to the center and contact with each other at $t = 0.85$. The values of \hat{m} and \hat{j} are 12 and 9, respectively. Two DOFs are constrained at each of supports 2–5, i.e., $k = 8$, and 24 DOFs are released, i.e., $d = 24$. Therefore, the value of q obtained from Eq. (19) is

$6 \times 9 - 6 \times 12 + 24 - 8 = -2$, which means that the mechanism is overconstrained. To investigate more details, singular value decomposition is carried out for \mathbf{G} to find that the values of g_r , g_c , and r are 62, 72, and 61, respectively; i.e., the structure has 11 statical indeterminacy and single-degree kinematic indeterminacy.

Note that the hinges at nodes 6–9 are inclined in diagonal directions. The number of hinges is 24, while 28 hinges are needed in the previous results by Ohsaki et al. (2014), where only the hinges in the directions of local axes are allowed.

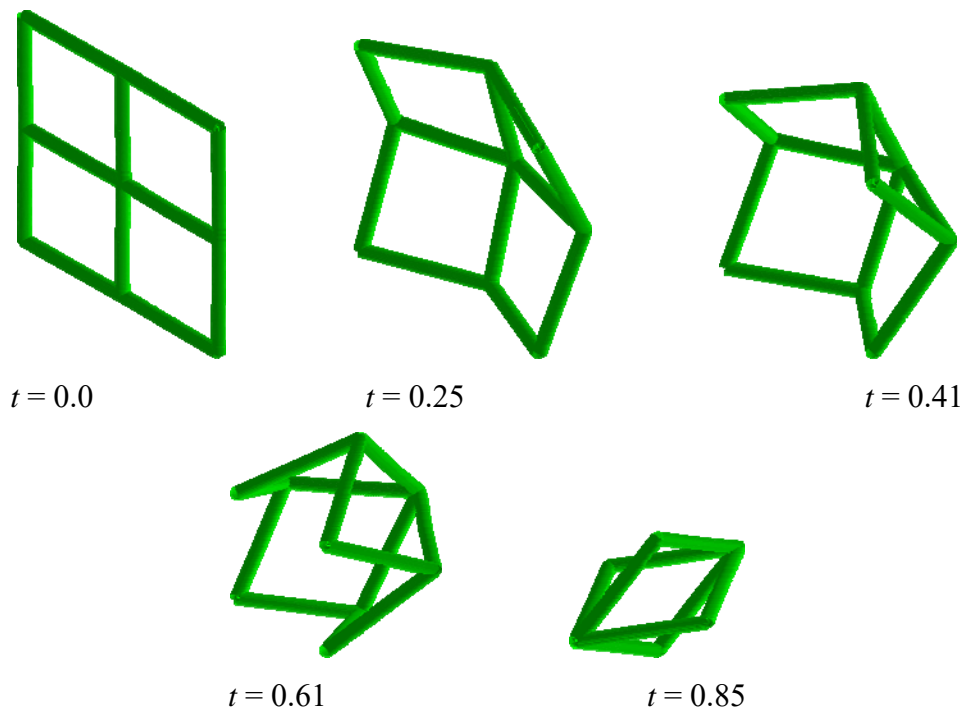


Figure 11: Deformation process of finite mechanism of Model 2 ($\alpha = 0.1$).

Model 3

Finally, we consider a 3-dimensional model as shown in Fig. 12. Nodal coordinates are listed in Table 3. Displacements are fixed in x - and z -directions at nodes 1 and 2, in x -direction at node 3, and in y -direction at node 7. The connectivities of 24 members are listed in Table 4.

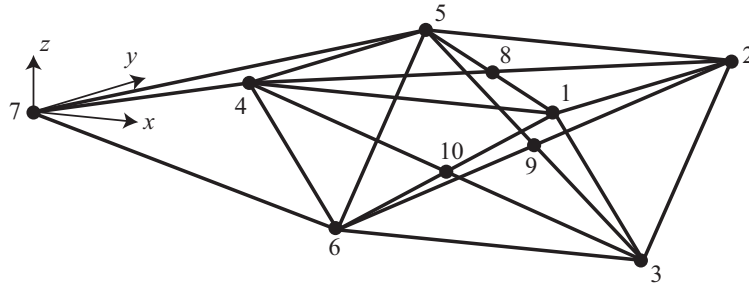


Figure 12: Diagonal view of a 3-dimensional model (Model 3).

Table 3: Nodal coordinates of Model 3.

Node	X	y	z
1	4.0	-1.0	0.5
2	4.0	1.0	0.5
3	4.0	0.0	-0.5
4	2.0	-1.0	0.5
5	2.0	1.0	0.5
6	2.0	0.0	-0.5
7	0.0	0.0	0.0
8	3.0	0.0	0.5
9	3.0	0.5	0.0
10	3.0	-0.5	0.0

Table 4: Connectivities of members of Model 3.

Member	Node a	Node b	Member	Node a	Node b
1	1	2	13	1	8
2	2	3	14	2	8
3	1	3	15	4	8
4	1	4	16	5	8
5	2	5	17	2	9
6	3	6	18	3	9
7	4	5	19	5	9
8	5	6	20	6	9
9	4	6	21	1	10
10	4	7	22	3	10
11	5	7	23	4	10
12	6	7	24	6	10

A mechanism is generated so that the output node 7 moves in negative z -direction as a result of moving nodes 1 and 2 in positive and negative y -directions, respectively; i.e., the distance between nodes 1 and 2 is decreased. The weight coefficients w_m and w_f are

10.0 and 1.0, respectively. A small value is given for w_f , because member removal is necessary for this model. Problem (15) is solved to find the load factor $\hat{\mu} = 3.1574$; i.e., $\alpha^L = 1/(3.1574)^2 = 0.1003$.

The input and output loads are applied to solve problem (3) for $\alpha = 0.2$. From the Lagrange multipliers at the optimal solution, it is found that members 1, 4, 5, 6, 13, and 14 are to be removed. As a result, members 15 and 16 are removed, because they have no effect on stiffness of the structure. The remaining members are shown in Fig. 13, where the dotted lines with numbers in parentheses are the removed members. Members 2, 3, 17, 18, 21, and 22, connecting nodes (2,3), (1,3), (2,9), (3,9), (1,10), and (3,10), respectively, have hinges at both member ends. The hinge directions in global coordinates are listed in Table 5.

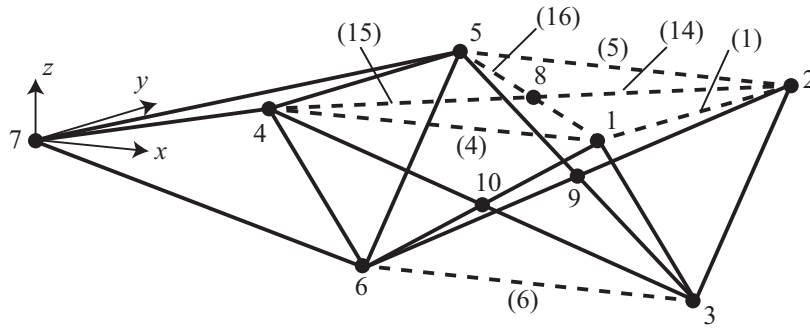


Figure 13: Remaining members of Model 3 after solving problem (3); dotted lines with numbers in parentheses: removed members.

Table 5: Hinge directions in global coordinates of Model 3.

Member	Node	X	y	z
2	2	0.20114	0.08385	-0.39053
	3	-0.11373	-0.17126	-0.39716
3	1	0.20114	-0.08385	0.39053
	3	-0.11373	0.17126	0.39716
17	2	-0.00228	-0.39570	-0.20838
	9	-0.01829	-0.39976	-0.19964
18	3	0.33734	-0.13130	-0.26261
	9	0.44373	-0.02491	-0.04982
21	1	-0.00228	0.39570	0.20838
	10	-0.01829	0.39976	0.19964
22	3	0.33734	0.13130	0.26261
	10	0.44373	0.02491	0.04982

Large-deformation analysis is carried out using ABAQUS. Each member has pipe cross-section with radius 10 mm and thickness 1 mm. Forced displacements of 0.4 m and -0.4 m in x -direction are given at nodes 1 and 2, respectively, while the path-parameter t is increased from 0 to 1. Deformation at $t = 0.0, 0.3, 0.5,$ and 1.0 , when the output displacement is 0.0, 0.3182, 0.4710, and 0.7151, respectively, are shown in Fig. 14.

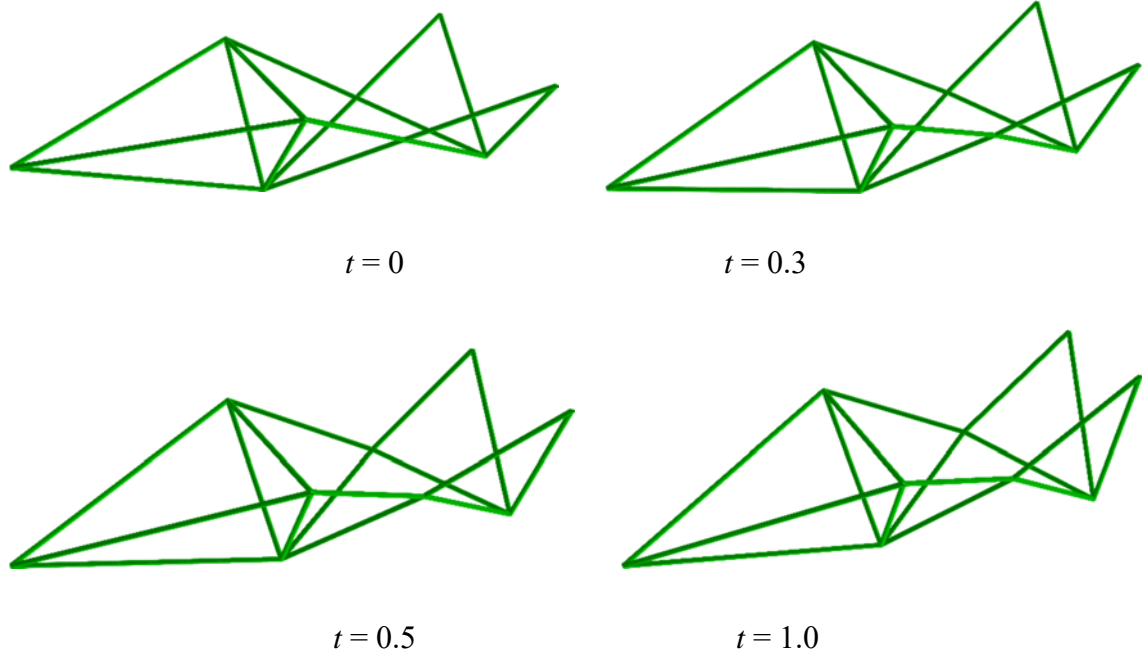


Figure 14: Deformation process of Model 3.

The linkage mechanism obtained by solving problem (3) has 9 nodes and 16 members, i.e., $\hat{m}=16$, $\hat{j}=9$. Two DOFs are constrained at nodes 1 and 2, and one DOF is constrained at nodes 3 and 7, i.e., $k=6$, and 12 DOFs are released, i.e., $d=12$. Therefore, the value of q obtained from Eq. (19) is $6 \times 9 - 6 \times 16 + 12 - 6 = -36$. However, the rigid part consisting of 10 members 7–12, 19, 20, 23, and 24 can be replaced by rigidly connected two members between nodes 7 and 9 as well as nodes 7 and 10. Therefore, the value of q reduces to 0. However, we found from singular value decomposition that the values of g_r , g_c , and r are 60, 90, and 59, respectively; i.e., the structure has 31 statical indeterminacy and single-degree kinematic indeterminacy.

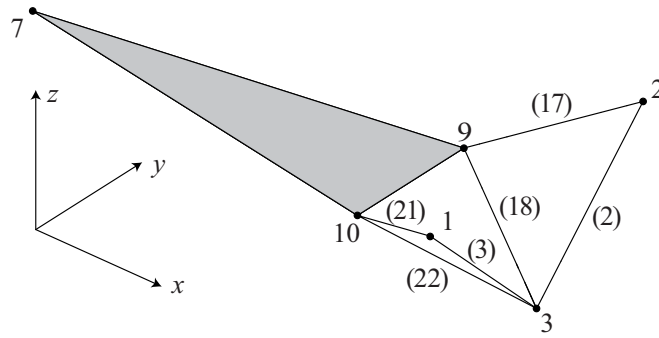


Figure 15: Simplified mechanism of Model 3; numbers in parentheses: remaining members.

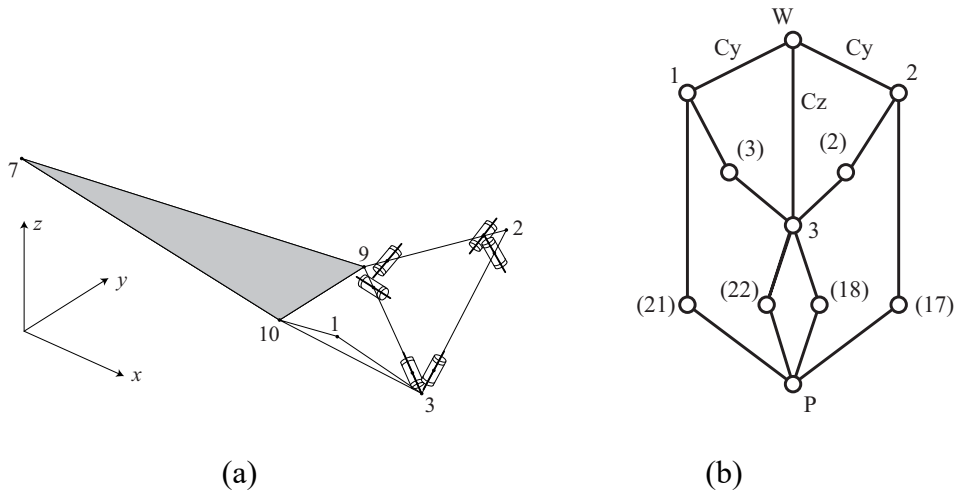


Figure 16: Kinematic chain of simplified mechanism of Model 3; (a) 3-dimensional model (revolute joints in members 3, 21, and 22 connecting nodes (1,3), (1,10), and (3,10), respectively, are not shown); (b) graphical representation; ‘P’: triangular plate, ‘W’: wall containing nodes 1, 2, and 3; Cy and Cz: cylindrical joints along y- and z-axes, respectively; line without any notation: revolute joint; numbers with and without parentheses: member numbers and node numbers, respectively.

We replace the rigid part consisting of nodes 7, 9, and 10 by a rigid triangular plate defined by nodes 7, 9, and 10 as shown in Fig. 15. Suppose nodes 1, 2, and 3 are attached to a wall through cylindrical joints to restrict rigid-body motions. The 3-dimensional model of the kinematic chain associate with this mechanism is shown in Fig. 16(a), where the revolute joints in members 3 and 21 connecting nodes (1,3) and (1,10), respectively,

are not shown for clarity of presentation. The graphical representation is drawn in Fig. 16(b), where ‘P’ is the triangular plate, ‘W’ is the wall containing nodes 1, 2, and 3, and C_y and C_z are the cylindrical joints along y - and z -axes, respectively. The line without any notation represents a revolute joint. The numbers with and without parentheses are member numbers and node numbers, respectively.

5. Conclusions

A new method has been presented for generating a mechanism by solving a quadratic programming problem. The following conclusions are obtained from this study:

1. A mechanism with hinges in arbitrarily inclined directions can be found by solving a quadratic programming problem. The problem is regarded as a limit analysis problem with quadratic yield functions of the member-end moments and axial force. The plastic hinge is regarded as a revolute joint in a linkage mechanism. A member is removed if the yield condition for member force is satisfied with equality. This way, a frame with partially released joints with small numbers of hinges and members can be obtained.
2. The hinge directions are obtained from the optimality conditions of the quadratic programming problem. Since the lower bound theorem is used, the variables are member-end moments and axial force. The nodal displacements and generalized strains including the hinge rotation and member extension are obtained as the Lagrange multipliers at the optimal solution. It is theoretically derived from the optimality conditions that the components of a hinge direction vector are proportional to the member-end moments and the magnitude of rotation is equal to the value of the generalized strain.
3. Since only small deformation is considered in the problem formulation, large deformation analysis should be carried out to add some hinges, if necessary, to generate a finite mechanism. By allowing inclined hinges, the number of hinges can be reduced from the results of the previous study, where only the hinges around the local axes are allowed.

References

- Artobolevsky, A., 1977. *Mechanisms in Modern Engineering Design*. MIR Publishers, Moscow.
- Chen, Y. You, Z., Tarnai, T., 2005. Three-fold-symmetric Bricard linkages for deployable structures. *Int. J. Solids. Struct.* 42, 2287–2301.
- Dassault Systèmes, 2014. *ABAQUS User's Manual Ver. 6.13*.
- Erdman, A.G., 1981. Three and four precision point kinematic synthesis of planar linkages. *Mechanism and Machine Theory*. 16, 227–245.
- Fowler, P.W., Guest, S.D., 2000. A symmetry extension of Maxwell's rule for rigidity of frames. *Int. J. Solids. Struct.* 37, 1793–1804.
- Erdman, A.G., 1995. Computer-aided mechanism design: Now and the future. *J. Mech. Des.*, ASME. 117(B), 93–100.
- Freudenstein, F., 1995. Approximate synthesis of four-bar linkages. *Trans. ASME*. 77, 853–861.
- Gill P.E., Murray W., Saunders M.A., 2002. SNOPT: An SQP algorithm for large-scale constrained optimization. *SIAM J. Opt.* 12, 979–1006.
- Guest, S.D., Fowler, P.W., A symmetry-extended mobility rule. *Mechanism and Machine Theory*. 40, 1002–1014.
- Kangwai, R.D., Guest, S.D., 1999. Detection of finite mechanisms in symmetric structures. *Int. J. Solids. Struct.* 36, 5507–5527.
- Kawamoto, A., Bendsøe, M.P., Sigmund, O., 2004. Articulated mechanism design with a degree of freedom constraint. *Int. J. Numer. Meth. Eng.* 61, 1520–1545.
- Kim, Y.Y., Jang, G.-W., Park, J.H., Hyun, J.S., Namm, S.J., 2007. Automatic synthesis of a planar linkage mechanism with revolute joints by using spring-connected rigid block models. *J. Mech. Des.*, ASME. 129, 930–940.
- Kovács, F., Tarnai, T., Fowler, P.W., Guest, S.D., 2004. A class of expandable polyhedral structures. *Int. J. Solids. Struct.* 41, 1119–1137.
- Krishnamurty, S., Turcic, D.A., 1992. Optimal synthesis of mechanisms using nonlinear goal programming techniques. *Mechanism and Machine Theory*. 27, 599–612.

- Liu, R., Phillippe, S., Rameau, J.-F., 2013. A tool to check mobility under parameter variations in over-constrained mechanisms. *Mechanism and Machine Theory*. 69, 44–61.
- Luo, Y., Yu, Y., Liu, J., 2008. A retractable structure based on Bricard linkages and rotating rings of tetrahedra. *Int. J. Solids. Struct.* 45, 620–630.
- MathWorks, 2013. *Matlab User's Manual Ver. R2013a*.
- Ohsaki M., Kanno Y., Tsuda S., 2014. Linear programming approach to design of spatial link mechanism with partially rigid joints. *Struct. Multidisc. Optim.* 50, 945–956.
- Olson, D.G., Erdman, A.G., Riley, D.R., 1985. A systematic procedure for type synthesis of mechanisms with literature review. *Mechanism and Machine Theory*. 20, 285–295.
- Patel, J., Ananthasuresh, G.K., 2007. A kinematic theory for radially foldable planar linkages. *Int. J. Solids. Struct.* 44, 6279–6298.
- Root, R.R., Ragsdell, K.M., 1976. A survey of optimization methods applied to the design of mechanisms. *J. Eng. for Industry, ASME*. 98, 1036–1041.
- Schulze, B., Guest, S.D., Fowler, P.W., 2014. When is a symmetric body-hinge structure isostatic?. *Int. J. Solids. Struct.* 51, 2157–2166.
- Shames, I.H., Cozzarelli, F.A., 1997. *Elastic and Inelastic Stress Analysis*. Taylor and Francis.
- Stolpe, M., Kawamoto, A., 2005. Design of planar articulated mechanisms using branch and bound. *Mathematical Programming*. 103, 357–397.
- Tsuda S., Ohsaki M., Kanno Y., 2013a. Analysis and design of deployable frames with partially rigid connections. *Proc. IASS Symposium 2013, Wroclaw, Poland, Int. Assoc. Shell and Spatial Struct., Paper No. 1206*.
- Tsuda S., Ohsaki M., Kikugawa S., Kanno Y., 2013b. Analysis of stability and mechanism of frames with partially rigid connections. *J. Struct. Constr. Eng., AIJ*, 78(686), 791–798. (in Japanese)

Yan, X.-F., Zhou, L., Duan, Y.-F., 2012. Singularity and kinematic bifurcation analysis of pin-bar mechanisms using analogous stiffness method. *Int. J. Solids. Struct.* 49, 1212–1226.

Zhang, C., Norton, R.L., Hammonds, T., 1984. Optimization of parameters for specified path generation using an atlas of coupler curves of geared five-bar linkages. *Mechanism and Machine Theory*. 19, 459–466.

Appendix

A1. Derivation of equilibrium matrix

The shear forces in the directions of local coordinates 2 and 3 at member-end a of member k are defined as $Q_{a2}^{(k)}$ and $Q_{a3}^{(k)}$, respectively, as shown in Fig. A1. The shear forces $Q_{b2}^{(k)}$ and $Q_{b3}^{(k)}$ at member-end b are defined similarly.

Let $L^{(k)}$ denote the length of member k . From equilibrium conditions of the member, the following equations are to be satisfied:

$$\begin{aligned}
 Q_{a2}^{(k)} + Q_{b2}^{(k)} &= 0 \\
 Q_{a3}^{(k)} + Q_{b3}^{(k)} &= 0 \\
 Q_{a2}^{(k)} L^{(k)} - M_{a3}^{(k)} - M_{b3}^{(k)} &= 0 \\
 Q_{a3}^{(k)} L^{(k)} + M_{a2}^{(k)} + M_{b2}^{(k)} &= 0
 \end{aligned}
 \tag{A1}$$

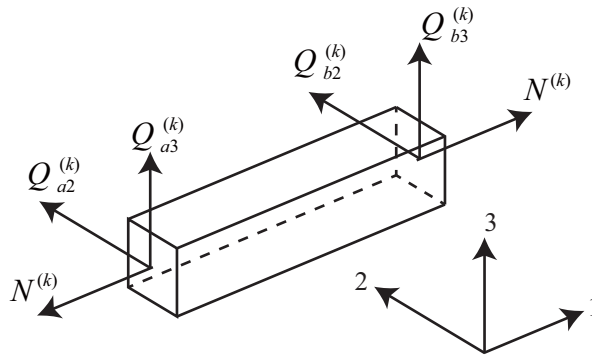


Figure A1: Definition of member-end shear forces.

Let $p_{ai}^{(k)}$ denote the nodal load at node a in the direction of local coordinate i of member k . The moments about the axis of local coordinate i is denoted by $m_{ai}^{(k)}$. The loads $p_{bi}^{(k)}$ and moments $m_{bi}^{(k)}$ at node b are defined similarly. From Eq. (A1), the shear forces $Q_{a2}^{(k)}$, $Q_{b2}^{(k)}$, $Q_{a3}^{(k)}$, and $Q_{b3}^{(k)}$ are expressed in terms of $M_{a2}^{(k)}$, $M_{b2}^{(k)}$, $M_{a3}^{(k)}$, and $M_{b3}^{(k)}$, and the following equilibrium equation is derived:

$$\begin{pmatrix} p_{a1}^{(k)} \\ p_{a2}^{(k)} \\ p_{a3}^{(k)} \\ m_{a1}^{(k)} \\ m_{a2}^{(k)} \\ m_{a3}^{(k)} \\ p_{b1}^{(k)} \\ p_{b2}^{(k)} \\ p_{b3}^{(k)} \\ m_{b1}^{(k)} \\ m_{b2}^{(k)} \\ m_{b3}^{(k)} \end{pmatrix} = \begin{pmatrix} -1 & 0 & 0 & 0 & 0 & 0 \\ 0 & 0 & 0 & 1/L^{(k)} & 0 & 1/L^{(k)} \\ 0 & 0 & -1/L^{(k)} & 0 & -1/L^{(k)} & 0 \\ 0 & -1 & 0 & 0 & 0 & 0 \\ 0 & 0 & 1 & 0 & 0 & 0 \\ 0 & 0 & 0 & 1 & 0 & 0 \\ 1 & 0 & 0 & 0 & 0 & 0 \\ 0 & 0 & 0 & -1/L^{(k)} & 0 & -1/L^{(k)} \\ 0 & 0 & 1/L^{(k)} & 0 & 1/L^{(k)} & 0 \\ 0 & 1 & 0 & 0 & 0 & 0 \\ 0 & 0 & 0 & 0 & 1 & 0 \\ 0 & 0 & 0 & 0 & 0 & 1 \end{pmatrix} \begin{pmatrix} N^{(k)} \\ T^{(k)} \\ M_{a2}^{(k)} \\ M_{a3}^{(k)} \\ M_{b2}^{(k)} \\ M_{b3}^{(k)} \end{pmatrix} \quad (\text{A2})$$

which is written in a matrix-vector form as

$$\mathbf{p}^{(k)} = \mathbf{H}^{(k)} \mathbf{f}^{(k)} \quad (\text{A3})$$

Eq. (A3) is transformed to the global coordinates, and assembled to derive the equilibrium equation (1).